



 Latest updates: <https://dl.acm.org/doi/10.1145/3714394.3756245>

RESEARCH-ARTICLE

Toward High Spatial Resolution and Low Ambiguity in Wideband Signal Receiver Beamforming for VR/AR

LONGYUAN GE, Shanghai Jiao Tong University, Shanghai, China

JUNTAO ZHOU, Shanghai Jiao Tong University, Shanghai, China

DIAN DING, Shanghai Jiao Tong University, Shanghai, China

YICHAO CHEN, Shanghai Jiao Tong University, Shanghai, China

YU LU, Shanghai Jiao Tong University, Shanghai, China

YIDA WANG, Shanghai Jiao Tong University, Shanghai, China

[View all](#)

Open Access Support provided by:

Shanghai Jiao Tong University



PDF Download
3714394.3756245.pdf
19 January 2026
Total Citations: 0
Total Downloads: 85

Published: 12 October 2025

[Citation in BibTeX format](#)

UbiComp '25: The 2025 ACM International Joint Conference on Pervasive and Ubiquitous Computing / ISWC ACM International Symposium on Wearable Computers
October 12 - 16, 2025
Espoo, Finland

Conference Sponsors:
SIGMOBILE
SIGCHI

Toward High Spatial Resolution and Low Ambiguity in Wideband Signal Receiver Beamforming for VR/AR

Longyuan Ge

gly2000@sjtu.edu.cn

Shanghai Jiao Tong University

Shanghai, China

Yi-Chao Chen

yichao@sjtu.edu.cn

Shanghai Jiao Tong University

Shanghai, China

Juntao Zhou

juntaozhou@sjtu.edu.cn

Shanghai Jiao Tong University

Shanghai, China

Yu Lu

yulu01@sjtu.edu.cn

Shanghai Jiao Tong University

Shanghai, China

Dian Ding

yichao@sjtu.edu.cn

Shanghai Jiao Tong University

Shanghai, China

Yida Wang

yidawang@sjtu.edu.cn

Shanghai Jiao Tong University

Shanghai, China

Guangtao Xue

gt_xue@sjtu.edu.cn

Shanghai Jiao Tong University

Shanghai, China

Abstract

Accurate angle of arrival (AoA) estimation is critical for virtual and augmented reality applications, as it enhances auditory cues and enables immersive sound-based interactions. However, traditional receiver beamforming methods for AoA estimation using fixed microphone arrays struggle to achieve both high spatial resolution and low ambiguity, especially across wide frequency ranges. In this paper, we propose a novel receiver beamforming system that employs a dynamically reconfigurable circular microphone array with an adjustable radius, paired with a frequency-adaptive ambiguity suppression algorithm. This flexible design allows our system to maintain high spatial resolution, suppress ambiguity lobes effectively, and deliver consistent accuracy across a wide frequency range. Experimental evaluations demonstrate that our system surpasses traditional approaches, delivering superior accuracy, robustness, and adaptability in complex acoustic environments.

CCS Concepts

• Human-centered computing → Ubiquitous and mobile computing.

Keywords

AoA Estimation; Beamforming Algorithm; Microphone Array

ACM Reference Format:

Longyuan Ge, Juntao Zhou, Dian Ding, Yi-Chao Chen, Yu Lu, Yida Wang, and Guangtao Xue. 2025. Toward High Spatial Resolution and Low Ambiguity in Wideband Signal Receiver Beamforming for VR/AR. In *Companion of the 2025 ACM International Joint Conference on Pervasive and Ubiquitous Computing (UbiComp Companion '25)*, October 12–16, 2025, Espoo, Finland. ACM, New York, NY, USA, 5 pages. <https://doi.org/10.1145/3714394.3756245>

Permission to make digital or hard copies of all or part of this work for personal or classroom use is granted without fee provided that copies are not made or distributed for profit or commercial advantage and that copies bear this notice and the full citation on the first page. Copyrights for components of this work owned by others than the author(s) must be honored. Abstracting with credit is permitted. To copy otherwise, or republish, to post on servers or to redistribute to lists, requires prior specific permission and/or a fee. Request permissions from permissions@acm.org.

UbiComp Companion '25, Espoo, Finland

© 2025 Copyright held by the owner/author(s). Publication rights licensed to ACM.

ACM ISBN 979-8-4007-1477-1/2025/10

<https://doi.org/10.1145/3714394.3756245>

the 2025 ACM International Joint Conference on Pervasive and Ubiquitous Computing (UbiComp Companion '25), October 12–16, 2025, Espoo, Finland. ACM, New York, NY, USA, 5 pages. <https://doi.org/10.1145/3714394.3756245>

1 Introduction

Accurate acoustic angle of arrival (AoA) estimation plays a vital role in enriching multimodal sensory input for virtual reality (VR) and augmented reality (AR) applications. In immersive environments, the ability to localize sound sources precisely enhances auditory cues and interactivity [3, 9, 13, 23]. By improving the spatial resolution and reliability of acoustic input, advanced receiver beamforming bridges the gap between auditory and visual modalities, enabling more precise and realistic VR/AR interactions.

Traditional AoA estimation systems typically use fixed microphone arrays [5, 10] and beamforming algorithms, such as the MUSIC algorithm [21]. However, the primary challenge lies in achieving an optimal balance between spatial resolution and ambiguity. To achieve a high spatial resolution, increasing the distance between the microphones is necessary. However, an increase in separation can result in the introduction of grating lobes, which are false peaks in the spectrum that cause ambiguity in the estimated AoA [14]. In the case of a fixed-frequency sound source, the distance between the microphones is typically set to half the wavelength. This issue becomes particularly problematic when the half-wavelength condition cannot be satisfied, as the dimensions of the microphone exceed half-wavelength. Moreover, fixed microphone configurations lack the ability to adapt to varying wavelengths, resulting in a reduction in resolution and an increase in ambiguity at specific frequencies [11]. Consequently, there is an increasing requirement for a more flexible and adaptable AoA estimation system that can maintain high accuracy in a range of VR/AR scenarios.

Our approach: We present a novel acoustic AoA estimation system that incorporates a dynamically adjustable circular microphone array configuration and a proposed ambiguity suppression algorithm. The system allows for dynamic control of the radius of the microphone array, which enables the fusion of AoA measurements with varying radius to achieve optimal spatial resolution while resolving the ambiguity of AoA measurements. Moreover, our approach

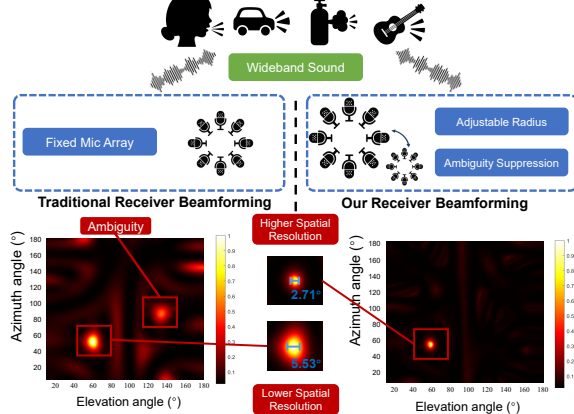


Figure 1: High spatial resolution and low ambiguity wideband beamforming for VR/AR applications via adaptive microphone array and ambiguity suppression.

utilizes a proposed ambiguity suppression algorithm which can be adapted to a variety of beamforming algorithms. In conclusion, our system provides a precise AoA estimation of varying sound frequencies, thereby significantly enhancing its applicability in complex environments. Our main contributions are outlined below:

- **Innovative Hardware Design:** We propose an adjustable circular microphone array system with dynamic radius control, distinguishing it from traditional fixed array systems. This design provides enhanced spatial resolution and adaptability across various sound frequencies, overcoming limitations of fixed frequency arrays in terms of performance consistency and applicability in diverse environments.
- **Ambiguity Suppression Algorithm:** We introduce an ambiguity suppression algorithm tailored to wideband signal processing, which minimizes grating lobes and ambiguity by integrating measurements from different microphone radii. This approach ensures clearer angle estimation and robust performance, even in complex acoustic environments.
- **Prototype and Comprehensive Performance Evaluation:** We developed a fully functional prototype of the proposed system and conducted extensive experiments that compare it with other array designs. The results demonstrate superior spatial resolution, reduced ambiguity, and overall precision, which confirms the effectiveness of the system in multiple acoustic scenarios.

2 Related Work

2.1 Design of Microphone Array

Many studies have optimized the design of microphone arrays for their application scenarios. [2], [26], and [28] use non-uniform array design to decrease ambiguity level. [7] increase the number of microphones and place them in different separations to improve performance against different sound frequencies. [6] uses a metasurface to manipulate sound waves to achieve the desired spatial properties. [25] places the microphone array on a mobile robot to introduce additional degrees of freedom and achieve more consistent performance across varying conditions and frequencies.

Our system enables the dynamic control of the microphone array instead of a fixed microphone configuration to maintain consistent performance over a wide frequency range.

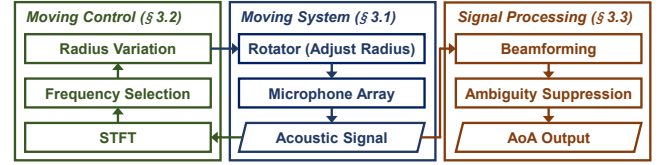


Figure 2: Architecture of our system.



(a) Inner Layer Bracket (b) Outer Layer Bracket (c) Adjust Radius

Figure 3: Brackets design.

2.2 Beamforming Algorithm

Receiver beamforming is a widely used method in sensing applications, particularly for estimating the AoA. Traditional beamforming methods [12, 15, 20, 21, 29, 30] for AoA estimation predominantly rely on array signal processing techniques. To improve the performance of traditional methods, tapering techniques [12, 30] and Taylor windowing [15] have been used to achieve a trade-off between main lobe width and ambiguity suppression. In recent years, unlike traditional methods that rely on mathematical models and assumptions about the environment, neural networks [1, 6, 18, 27] can learn directly from data, making them adaptable to different acoustic environments.

These algorithms estimate AoA based on differences in sound signals from microphones at different locations. Therefore, these algorithmic improvements do not conflict with our system. Our system can be adapted to a variety of beamforming algorithms.

3 System Design

In this section, we propose our adjustable circular microphone array system to achieve high spatial resolution, low ambiguity, and wideband signal beamforming. Fig.2 illustrates the architecture. Our system consists of three parts: 1) a moving system to adjust the radius of the uniform circular microphone array; 2) a moving control strategy to decide how to adjust the radius; and 3) a receiver beamforming for spectrum generation and ambiguity suppression.

3.1 Moving System

The moving system consists of two primary layers of circular brackets. The inner layer is immovable and has straight guide slots, as shown in Fig. 3(a). The outer layer can rotate around the center and has arc-shaped guide slots, as shown in Fig. 3(b). The microphones are confined simultaneously in the guide slots of the two layers of brackets at the intersection of the slots, as shown in Fig. 3(c). The guide slots on the outer layer bracket can be described as:

$$x = \{r_{\min} + \frac{(r_{\max} - r_{\min})\theta}{\theta_{\max}}\} \cos \theta \quad (1)$$

$$y = \{r_{\min} + \frac{(r_{\max} - r_{\min})\theta}{\theta_{\max}}\} \sin \theta \quad (2)$$

where r_{\min} and r_{\max} are the minimum and maximum radii of the microphone array, and θ_{\max} is the maximum rotation angle.

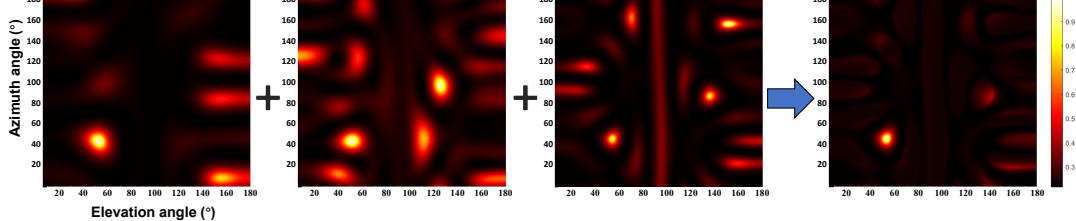


Figure 4: An example of applying the ambiguity suppression algorithm to combine spectrums. Ambiguity lobes are removed from spectrums generated at different radii, leaving only the main lobe after this operation.

3.2 Moving Control

3.2.1 Frequency Selection. After recording the incoming sound, short-time fourier transform (STFT) [8] is performed first to analyze the frequency component of the sound sources. In this way, we can decompose the received sound into the sum of the signals of different frequency bands. Then, a bandpass filter is applied to target specific signal components.

3.2.2 Radius Variation Strategy. To achieve high spatial resolution, it is necessary to increase the radius between the microphones. However, an increase in separation can result in the introduction of grating lobes. We set the radius to the minimum first. Then we gradually increase the radius and record the signals. After a measurement, the radius returns to the minimum.

3.3 Signal Processing

3.3.1 Beamforming. After targeting specific signal components, we use a beamforming algorithm to generate the spectrums. For each selected frequency f , we can compute the MUSIC spectrum[21] over a grid of possible angles (θ, ϕ) by

$$P_{\text{MUSIC}}(\theta, \phi) = \frac{1}{\mathbf{a}^H(\theta, \phi) \mathbf{U}_n \mathbf{U}_n^H \mathbf{a}(\theta, \phi)} \quad (3)$$

where $\mathbf{a}(\theta, \phi)$ is the steering vector and \mathbf{U}_n is the noise subspace matrix determined by received signals. The location of these peaks in the (θ, ϕ) spectrum corresponds to the estimated AoA of the sound source. Note that the AoA (θ, ϕ) only influences the propagation path difference between the microphones, and the MUSIC algorithm can be replaced by other beamforming algorithms.

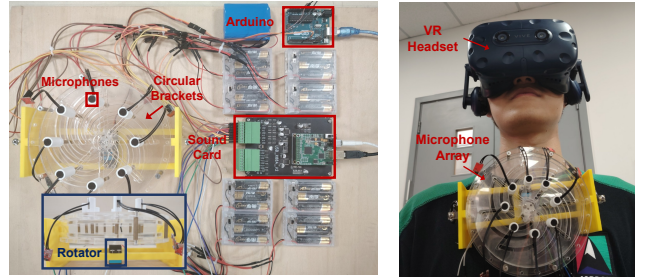
3.3.2 Ambiguity Suppression. To mitigate the effects of ambiguity lobes, we propose an ambiguity suppression algorithm that combines the spectrums obtained from different radii. Given the spectrum $P_i(\theta, \phi)$ obtained from the i -th configuration of radius r_i , the combined spectrum $P_{\text{combined}}(\theta, \phi)$ is defined as:

$$P_{\text{combined}}(\theta, \phi) = \sum_i w_i P_i(\theta, \phi) \quad (4)$$

where w_i is the weight of the i -th spectrum estimation $P_i(\theta, \phi)$, indicating the confidence in that estimation. Inspired by maximum ratio combining (MRC) in wireless communication [22, 24], we set w_i as the inverse of the estimation variance:

$$w_i = \frac{P_i(\theta, \phi)}{\sum_j (P_j(\theta, \phi))} \quad (5)$$

As shown in Fig. 4, the ambiguity suppression algorithm effectively cancels out grating lobes, which shift with changes in r_i while the main lobe remains fixed. Additionally, some noise-induced ambiguity lobes are also weakened, as their random positions vary across multiple measurements, reducing their impact in the combined spectrum.



(a) Hardware Implementation (b) Compatible with VR Headset

Figure 5: System prototype.

4 Implementation & Evaluation

4.1 Implementation

As shown in Fig.5(a), our system's hardware consists of three main parts: an 8-channel microphone array, circular brackets, and a rotator. All of these parts are connected to a laptop with an Intel I7 processor and 16 GB of memory. The control and processing are performed using MATLAB [16]. As shown in Fig.5(b), our system is compatible with a VR headset.

4.1.1 Microphone Array. We use a USB ASIO 8 channel sound card with a sampling rate of 192kHz to record the sound signal from the microphones. The microphone (MAX4466 [17]) is a condenser electret microphone module with an integrated operational amplifier. The microphones can move along the guide slots on the brackets.

4.1.2 Circular Brackets. The circular brackets are constructed from 3D-printed support bases and laser-cut acrylic skeletons. To enhance the reliability of the structure, the system employs two sets of brackets. The inner layer brackets are fixed to the support bases. The outer layer brackets are connected to the rotator at the bottom.

4.1.3 Rotator. The rotator is a DS3235 motor servo [4] controlled by an Arduino mainboard. The Arduino mainboard controls the motor to rotate at a specified angle by sending pulse width modulation signals. In one measurement, the total time required to adjust the radius from 2cm to 5cm is less than 0.8s.

4.2 Evaluational Setup

In the experiment, we place our system on the floor of a 7m×7m×3m indoor room. Ambient noises include a constantly working air conditioner, people talking and footsteps, and some animals outside. We place a commercial speaker 2 meters away to play the sound. The SNR of the received acoustic signal remains consistent across all experiments by adjusting the speaker volume.

In order to evaluate our system, we design the following main evaluation indicators: (1) **ME**: Mean Error between the estimated AoA and the ground truth. ME is defined as the mean of the square root of the azimuth and elevation estimation errors. (2) **NMP** [14]: The Normalized Maximum ambiguity Peak, defined as the ratio

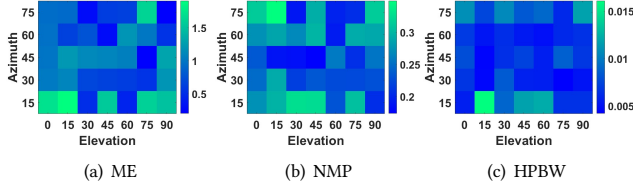


Figure 6: Preliminary performance evaluation of our system across varying azimuth and elevation angles.

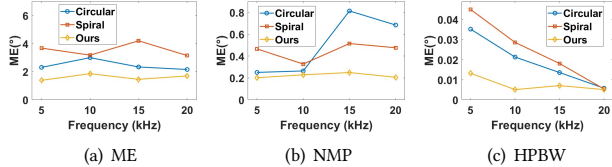


Figure 7: Comparison of AoA performance with other 2D array designs (Circular, Spiral).

of the highest ambiguity peak magnitude to the main lobe peak magnitude. A low NMP value indicates minimal ambiguity. (3) **HPBW** [19]: The Half-Power BeamWidth of the main lobe. HPBW is defined as the solid angle corresponding to the region where the magnitude exceeds half-power. A low HPBW indicates a narrow main lobe and high spatial resolution.

4.3 Performance

4.3.1 Initial Performance Assessment. To understand the basic performance of the proposed system, we set the sound source frequency to 15kHz and varied the azimuth and elevation angles in 15° increments for each test. As illustrated in Fig. 6, our system achieved an AoA estimation error below 1.9° , a NMP value under 0.35 , and an HPBW below 0.016 . These results demonstrate that our prototype successfully achieves high spatial resolution and effective ambiguity suppression across a range of angles.

4.3.2 Comparison to Existing Array Designs. To demonstrate the advantages of our system, we compared it against two established array designs at four different frequencies (5kHz , 10kHz , 15kHz , and 20kHz). The first design is a uniform Circular array with a 4cm radius. The effectiveness of a reconfigurable design can be demonstrated in comparison. The second design is a Spiral array with radii increasing from 2cm to 5.5cm . This non-uniform design is often studied for its ability to suppress ambiguity and improve spatial resolution over a wide frequency range. All arrays used 8 microphones. As shown in Fig. 7, our system achieved estimation errors that were 34.2% and 53.8% lower than those of the Circular and Spiral arrays, respectively. Similarly, NMP values in our system were reduced by 42.9% and 48.7% relative to the Circular and Spiral designs. Our system's HPBW was also narrower by 49.6% and 54.8% compared to these arrays. The results suggest that our system consistently achieved the lowest AoA estimation error, minimal ambiguity, and narrowest main lobes across all test frequencies.

4.4 Case Study

To evaluate the performance of our system in complex environments, we simulated an industrial maintenance scenario. In this setup, three machines make sounds in the factory: a cutting machine *A* generates continuous operational noise centered around 7kHz , a packaging machine *B* sounds an alarm at 4kHz due to a malfunction, and a compressor machine *C* exhibits a high-frequency

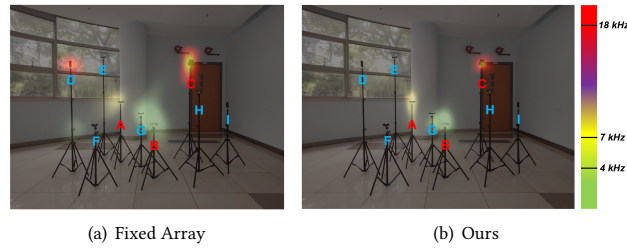


Figure 8: A simulated remote industrial maintenance scenario: A) 7kHz Cutting machine, B) 4kHz Urgent alarm, C) 18kHz Gas leakage, and D-I) Other quiet machines.

gas leakage at 18kHz . The microphone array collects sound signals, and the camera on the VR headset captures images. After calculation, a real-time spatialized sound map is generated and displayed on the engineer's VR headset. As shown in Fig. 8, the fixed array cannot effectively remove the ambiguity peaks from the high-frequency sound spectrum. This results in machine *D* being misjudged as gas leakage. The fixed array also has a relatively low spatial resolution for low-frequency sounds, with a large main lobe width that covers machines *B* and *G*. This will cause engineers to mistakenly believe that the quiet machine *G* is also sounding an alarm. Meanwhile, our system achieves fewer misjudgments due to higher spatial resolution and lower ambiguity.

5 Applications

This novel acoustic AoA estimation system has significant potential for use in various VR/AR applications.

Virtual Meeting: Our system has a higher spatial resolution, enabling it to more accurately determine the direction of each participant's voice. This enables spatial audio rendering that mimics real-world conversations.

Visual Assistance for the Hearing Impaired: This system can provide more accurate real-time visual prompts for users with hearing impairments because it can effectively eliminate ambiguity. **Industrial Inspection:** In AR-assisted industrial settings, this system can identify the source of abnormal sounds, such as leaks, vibrations, and mechanical faults. Factory sound frequency ranges are very wide, and our system can adapt to wideband signals.

6 Conclusion & Future work

This paper presents a novel receiver beamforming system that leverages a dynamically adjustable microphone array to improve spatial resolution and suppress ambiguity across a wide frequency range. By integrating adjustable radius with a novel ambiguity suppression algorithm, our system achieves consistent accuracy, outperforming traditional AoA estimation methods. Comprehensive evaluations demonstrate that our approach effectively addresses the limitations of fixed-array designs, providing enhanced robustness, adaptability, and precision in complex acoustic environments. These advancements make our system well-suited for VR/AR applications.

Future work will focus on miniaturizing the system for integration with VR/AR devices or for use as a portable peripheral. VR/AR interactions often involve the movement of either the human body or the devices themselves. Researchers can explore the potential of sensors that collect additional information during movement to enable more precise perception.

References

[1] Sharath Adavanne, Archontis Politis, and Tuomas Virtanen. 2018. Direction of arrival estimation for multiple sound sources using convolutional recurrent neural network. In *2018 26th European Signal Processing Conference (EUSIPCO)*. IEEE, 1462–1466.

[2] Elias JG Arcondoulis and Yu Liu. 2021. Acoustic beamforming array design methods over irregular shaped areas. *Journal of Vibration and Acoustics* 143, 3 (2021), 031013.

[3] Chao Cai, Henglin Pu, Peng Wang, Zhe Chen, and Jun Luo. 2021. We Hear Your PACE: Passive Acoustic Localization of Multiple Walking Persons. *Proc. ACM Interact. Mob. Wearable Ubiquitous Technol.* 5, 2, Article 55 (jun 2021), 24 pages.

[4] DS3235 2025. DS3235 Datasheet. https://github.com/microrobotics/DS3235-270/blob/master/DS3235-270_datasheet.pdf.

[5] Georg K.J. Fischer, Niklas Thiedecke, Thomas Schaechtle, Andrea Gabbrielli, Fabian Höflinger, Alexander Stolz, and Stefan J. Rupitsch. 2024. Evaluation of Sparse Acoustic Array Geometries for the Application in Indoor Localization. *IEEE Journal of Indoor and Seamless Positioning and Navigation* 2 (2024), 263–274. doi:10.1109/JISPIN.2024.3476011

[6] Yongjian Fu, Yongzhao Zhang, Hao Pan, Yu Lu, Xinyi Li, Lili Chen, Ju Ren, Xiong Li, Xiaosong Zhang, and Yaoxue Zhang. 2024. Pushing the Limits of Acoustic Spatial Perception via Incident Angle Encoding. *Proceedings of the ACM on Interactive, Mobile, Wearable and Ubiquitous Technologies* 8, 2 (2024), 1–28.

[7] Edno Gentilho Jr, Paulo Rogerio Scalassara, and Taufik Abrão. 2020. Direction-of-arrival estimation methods: A performance-complexity tradeoff perspective. *Journal of Signal Processing Systems* 92, 2 (2020), 239–256.

[8] Daniel Griffin and Jae Lim. 1984. Signal estimation from modified short-time Fourier transform. *IEEE Transactions on acoustics, speech, and signal processing* 32, 2 (1984), 236–243.

[9] Ryosuke Hanahara, Itsuki Yonemura, Koji Yamamoto, Takuto Arai, Shuki Wai, Tatsuhiko Iwakuni, Daisei Uchida, and Naoki Kita. 2024. Leveraging Acoustic AoA to Enhance mmWave Beam Search-Based Blockage Prediction: An Experimental Study. *IEEE Transactions on Vehicular Technology* 73, 10 (2024), 15598–15608. doi:10.1109/TVT.2024.3412738

[10] Gongping Huang, Jacob Benesty, Israel Cohen, and Jingdong Chen. 2020. A simple theory and new method of differential beamforming with uniform linear microphone arrays. *IEEE/ACM Transactions on Audio, Speech, and Language Processing* 28 (2020), 1079–1093.

[11] David Kure, Vaclav Mach, Kristian Orlovsky, and Hassan Khaddour. 2013. Sound source localization with DAS beamforming method using small number of microphones. In *2013 36th International Conference on Telecommunications and Signal Processing (TSP)*. IEEE, 526–532.

[12] Oliver Lange and Bin Yang. 2010. Array geometry optimization for direction-of-arrival estimation including subarrays and tapering. In *2010 International ITG Workshop on Smart Antennas (WSA)*. IEEE, 135–142.

[13] Kejing Ma, Huyue Chen, Zhiyuan Wu, Xiangling Hao, Ge Yan, Wenbo Li, Lei Shao, Guang Meng, and Wenming Zhang. 2022. A wave-confining metasphere beamforming acoustic sensor for superior human-machine voice interaction. *Science Advances* 8, 39 (2022), ead9230. doi:10.1126/sciadv.adc9230

[14] Wenguang Mao, Mei Wang, Wei Sun, Lili Qiu, Swadhin Pradhan, and Yi-Chao Chen. 2019. Rnn-based room scale hand motion tracking. In *The 25th Annual International Conference on Mobile Computing and Networking*. 1–16.

[15] Cherian P Mathews and Michael D Zoltowski. 2002. Beamspace esprit for multi-source arrival angle estimation employing tapered windows. In *2002 IEEE International Conference on Acoustics, Speech, and Signal Processing*. Vol. 3. IEEE, III–3009.

[16] MATLAB 2025. MATLAB. <https://www.mathworks.com/products/matlab.html>.

[17] MAX4466 2025. MAX4466-Low-Cost, Micropower, SC70/SOT23-8, Microphone Preamplifiers with Complete Shutdown. <https://www.analog.com/en/products/max4466.html#part-details>.

[18] Weihang Nie, Xiaowei Zhang, Ji Xu, Lianghao Guo, and Yonghong Yan. 2023. Adaptive direction-of-arrival estimation using deep neural network in marine acoustic environment. *IEEE Sensors Journal* 23, 13 (2023), 15093–15105.

[19] Saeed Ur Rahman, Qunsheng Cao, Muhammad Mansoor Ahmed, and Hisham Khalil. 2017. Analysis of linear antenna array for minimum side lobe level, half power beamwidth, and nulls control using PSO. *Journal of Microwaves, Optoelectronics and Electromagnetic Applications* 16 (2017), 577–591.

[20] Richard Roy and Thomas Kailath. 1989. ESPRIT-estimation of signal parameters via rotational invariance techniques. *IEEE Transactions on acoustics, speech, and signal processing* 37, 7 (1989), 984–995.

[21] Ralph Schmidt. 1986. Multiple emitter location and signal parameter estimation. *IEEE transactions on antennas and propagation* 34, 3 (1986), 276–280.

[22] Amit Shah and Alexander M Haimovich. 2000. Performance analysis of maximal ratio combining and comparison with optimum combining for mobile radio communications with cochannel interference. *IEEE Transactions on Vehicular Technology* 49, 4 (2000), 1454–1463.

[23] Tokio Takada, Jin Nakazato, Alex Orsholits, Manabu Tsukada, Hideya Ochiai, and Hiroshi Esaki. 2024. Design of Digital Twin Architecture for 3D Audio Representation in AR. In *2024 IEEE International Conference on Metaverse Computing, Networking, and Applications (MetaCom)*. 222–230. doi:10.1109/MetaCom62920.2024.00044

[24] B.R. Tomiuk and N.C. Beaulieu. 2000. A new look at maximal ratio combining. In *Globecom '00 - IEEE, Global Telecommunications Conference. Conference Record (Cat. No.00CH37137)*. Vol. 2. 943–948 vol.2. doi:10.1109/GLOCOM.2000.891277

[25] Vladimir Tourbabin and Boaz Rafaely. 2015. Direction of arrival estimation using microphone array processing for moving humanoid robots. *IEEE/ACM Transactions on Audio, Speech, and Language Processing* 23, 11 (2015), 2046–2058.

[26] Temel Engin Tuncer, TK Yasar, and B Friedlander. 2007. Direction of arrival estimation for nonuniform linear arrays by using array interpolation. *Radio science* 42, 04 (2007), 1–11.

[27] Houhong Xiang, Baixiao Chen, Minglei Yang, Saiqin Xu, and Zhengjie Li. 2021. Improved direction-of-arrival estimation method based on LSTM neural networks with robustness to array imperfections. *Applied Intelligence* 51 (2021), 4420–4433.

[28] Zhengqin Xu, Shiqian Wu, Zhuliang Yu, and Xingyu Guang. 2019. A robust direction of arrival estimation method for uniform circular array. *Sensors* 19, 20 (2019), 4427.

[29] Yongzhao Zhang, Yezhou Wang, Lanqing Yang, Mei Wang, Yi-Chao Chen, Lili Qiu, Yihong Liu, Guangtao Xue, and Jiadi Yu. 2023. Acoustic Sensing and Communication Using Metasurface. In *20th USENIX Symposium on Networked Systems Design and Implementation (NSDI 23)*. 1359–1374.

[30] A Zielinski. 1987. An efficient method of Dolph-Chebyshev beamforming. In *Progress in underwater acoustics*. Springer, 759–764.